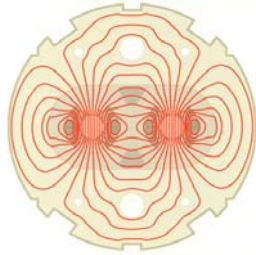


US/CERN LHC Accelerator Collaboration



DESIGN REPORT

for the

1.2. Interaction Region Dipoles

and the

2.1. RF Region Dipoles

Magnet Group

Brookhaven National Laboratory

September 3, 1999



Table of Contents

A. Introduction

B. Objectives, Specifications and Requirements

1. Overview
2. Dipole Cold Mass
3. Assembled Magnets

C. Technical Description

1. Superconductor
2. Dipole Beam Tube
3. Dipole Coil
4. Collars
5. Dipole Yoke and Helium Containment of the 2-in-1 Magnet
6. Analysis of the Collar-Yoke and the Yoke-Shell Interfaces
7. Electrical Connections and Quench Protection
8. Dipole Cryostats
9. Interfaces to LHC Systems and Magnet Cooling
10. Transfer Function, Quench Field, Inductance, and Stored Energy
11. Magnetic Field Quality - Measurements
12. Magnetic Field Quality – Measurement Errors
13. Magnetic Field Quality – Expected Values
14. Current Imbalance in the Left/Right Apertures
15. Magnet Shipping
16. Installation at CERN

D. R&D Program

E. Production Plan and Schedule

References

A. Introduction

The dipoles required in the Intersection Regions (IRs) of the LHC have field and aperture requirements close to those of the RHIC [1] arc dipole magnets. Thus the superconducting coils developed for those magnets can be used in a cost-effective dipole design that satisfies CERN's requirements. Under the auspices of the US/CERN LHC Collaboration, the required magnets will be built at BNL. Tooling constructed for the RHIC program will be used, so far as possible. RHIC magnets were built commercially but the company that built those magnets was not interested in this modest construction program. All magnets will be tested in the existing BNL cryogenic test facility, then shipped to CERN for installation in the LHC lattice. Close coordination is required between the two laboratories to ensure that they meet all requirements for operation in the LHC.

B. Objectives, Specifications and Requirements

B.1 Overview

The dipole magnets to be built will be a single aperture dipole labeled D1 and double aperture dipoles labeled D2, D3a, D3b, D4a, and D4b. The D1 magnet will be a single RHIC-type cold mass in a cryostat. The D3 magnets will be built with two single aperture RHIC-type cold masses in a single cryostat. The D2 and D4 magnets will be built as 2-in-1 cold masses in a single cryostat.

The D1 and D2 magnets bring the two beams of the LHC, separated by 194 mm in the arcs, into collision at four separate points, then separate the beams again beyond the collision point. The D2 magnets are specified for IRs 1, 2, 5 and 8. The D1 magnets will be used in IRs 2 and 8; for IRs 1 and 5, warm magnets not supplied by the US collaboration are planned. One side of one such region is shown in Figure 1.

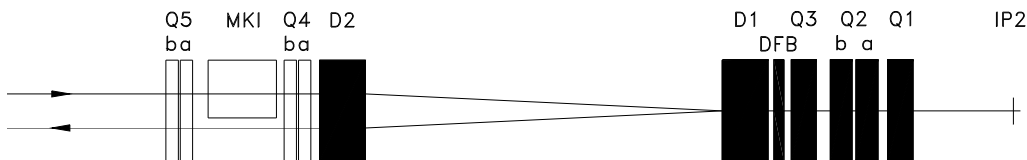


Figure 1 Geometry in Intersection Region 2 of the LHC. Dipole magnets D1 and D2 bring the beams into collision at IP2.

The D3 and D4 magnets increase the separation of the beams of the LHC from the nominal spacing of 194 mm to 420 mm so that individual RF cavities can be installed for each beam, and then return the beams to the nominal 194 mm spacing. This is planned for IR 4 of the LHC. A drawing of one side of this region is shown in Figure 2.

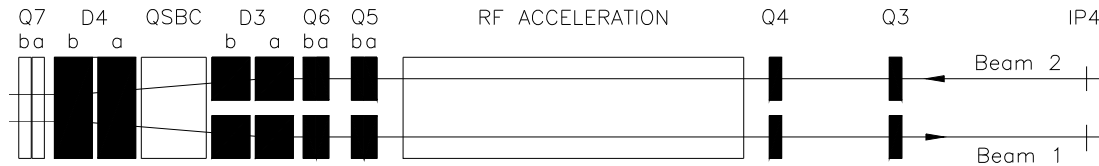


Figure 2 Geometry in the RF Region of the LHC. The nominal 194 mm separation of the beams is increased to 420 mm so that there is space for independent RF acceleration cavities for the two beams.

The dipole magnets are designed with a common element: superconducting coils that are mechanically the same as those built for the RHIC arc dipole magnets [1,2]. The RHIC dipole is a well understood magnet with good quench performance and field quality. The D1 magnets are designed with one RHIC-style cold mass in a cryostat and the D3 magnets are designed with two such cold masses side-by-side in a common cryostat. The cold masses are built straight, without the 47 mm sagitta of the RHIC magnets. The D2 and the D4 magnets are built with coils that are prestressed with stainless steel collars. These collared coils are assembled into yokes with common outside dimensions but with varying internal features (iron saturation control holes, aperture spacing) depending on location. The use of common outside dimensions reduces tooling cost. The yoke size has been constrained to fit into cryostats similar to those designed by CERN.

These 2-in-1 magnets have the field in each aperture in the same direction. This is different from the more usual 2-in-1 designs, such as used in the LHC arcs, where the fields are in opposite directions and the flux in one aperture returns through the other. With these in the same direction, the fields of the two apertures are decoupled and are like those in independent magnets, provided there is sufficient iron available to contain the flux. Judiciously placed cutouts in the yoke, where the placement is altered for each particular separation of the coil apertures, control the field asymmetries that would

otherwise be generated and minimize changes in the harmonics with excitation (field quality is discussed in Sections C.11 through C.14). Again, this latter goal is aided by having sufficient iron on the midplane to reduce saturation effects.

The field quality expected in these magnets is suitable for the LHC for nominal proton and heavy ion operation, both for injection and for collision lattices. This has been confirmed by Accelerator Physics tracking studies carried out as part of the US/CERN collaboration [3]. In these studies, both the dynamic aperture and the tune footprint were used as quantities to evaluate the impact of magnet errors.

The dipole magnets to be built by BNL for the LHC are summarized in Table 1.

Table 1 Dipole magnets to be built by Brookhaven for the LHC. The coil aperture is 80 mm. The overall length of the magnets is approximately 10 meters.

Name	Style	Number (Spares)	Aperture Separation (cold), mm	Operating Temperature, K
D1	Single Aperture	4(1)	---	1.9
D2	2-in-1	8(1)	188	4.5
D3a	Dual 1-in-1	2(1)	420	4.5
D3b	Dual 1-in-1	2(1)	382	4.5
D4a	2-in-1	2(1)	232	1.9
D4b	2-in-1	2(1)	194	1.9

Table 2 gives the magnetic field required in the various magnets for three values of the LHC energy: injection, nominal and 8 % above nominal.

Table 2 Position parameters and fields required in the magnets at injection energy, nominal energy, and 8% above nominal energy. The numbers listed for the bend center-to-center distance and the deflection are those specified in Version 6.0 of the LHC lattice. The magnetic length of the magnets is 9.45 m.

Magnet	IR Location	Bend Center-to-Center Distance, m	Deflection, m	Field (T) for E (TeV)		
				0.45	7.0	7.56
D2	1 & 5	87.432	0.097	0.1761	2.7393	2.9585
D1 or D2	2 left	62.697	0.097	0.2456	3.8201	4.1257
D1 or D2	2 right	66.062	0.097	0.2331	3.6255	3.9155
D1 or D2	8 left	65.582	0.097	0.2348	3.6520	3.9442
D1 or D2	8 right	62.522	0.097	0.2463	3.8308	4.1372
D3 or D4	4	39.100	0.113	0.2294	3.5679	3.8534

B.2 Dipole Cold Mass

The D3 magnets will be built as two side-by-side cold masses in a common cryostat. D3a cold masses will have center line separations of 420 mm and D3b cold masses will be separated by 382 mm. The cold masses will be similar to those in the main arc dipoles of RHIC, and the reader is referred to the RHIC Design Manual [1] for details on the design of this magnet. Some changes are necessary, however. The cold masses will be straight, not curved with a 47 mm sagitta as in RHIC. Quench protection heaters will be required so that the magnets can be protected from absorbing excessive energy in case they quench. This protection was provided by diodes in RHIC but these diodes are not suitable in the high radiation environment of the LHC. The two magnets for each beam will be cooled in series and each series loop will have independent connections to the cryogenic header. A substantial support cradle to hold two side-by-side cold masses on a common post is part of the design.

The D2 and D4 magnets will be built as 2-in-1 cold masses in which the two beam apertures are in a common yoke. This design allows the close spacing of the apertures required in the machine at those locations. The aperture spacings will be 188 mm for D2, 232 mm for D4a, and 194 mm for D4b. The necessary prestress cannot be applied to the coils with the yoke, however, as is done in the RHIC magnets. Therefore, stainless steel collars are used to apply the necessary prestress, and then the collared coils are installed side-by-side into the yoke, which is split on the horizontal mid-plane. The stainless steel collars are intended to constrain the full Lorentz forces when the magnet is powered. The laminated, cold steel yoke, encased in a stainless steel helium-containing cylinder, mechanically supports the coils. The helium vessel is also a structural part of the yoke assembly.

The cold masses will be installed into an LHC-diameter (0.914 m) vacuum containment. CERN will supply the support posts and the heat shield support extrusion. Brookhaven will build a heat shield that fits around the cold masses and will include the necessary cryogenic piping and its supports.

In the LHC, some of these magnets will be on an incline and cooled with a static bath of liquid helium operating at 1.3 bar, 4.5 K, as compared to RHIC where the magnets are

level and are cooled with single phase 5 bar, 4.5 K helium flowing at 100 g/s. To accommodate this cooling, the magnets must be fitted with vent pipes at their up-hill ends (which varies with position in the lattice) and with liquid level sensors in a suitably-sized volume. Piping in the cryostat is arranged to deliver helium to the down-hill end for initial cooling and at the uphill end for steady state operation, and to remove vapor at the up-hill end. The magnets can be operated at temperatures higher than 4.5 K to provide the required field; there is about a 3.5 % reduction in quench field with each 0.1 K temperature rise in this range.

In the lattice, these magnets are to be powered in series from a common power supply. This scheme is suitable for magnets that are all alike, because the magnet transfer functions could then be expected to be, within acceptable errors, close together in value. In the present design, however, this will not be the case. Even though the coils in the D3 and the D4 magnets will be the same, the different style of yoke surrounding the magnets will cause the required currents to differ by up to 400 A (~10 %) for a given field (see Section C.10). Several options exist for dealing with this difference; CERN will develop a strategy for accommodating it in powering the magnets.

Figure 3 shows cold mass cross sections for the four designs of magnets.

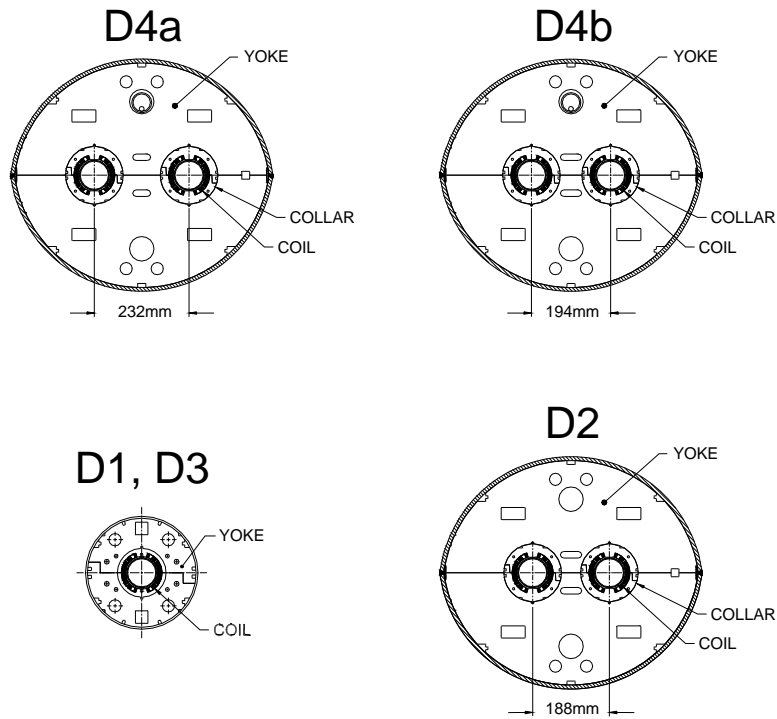


Figure 3 Cross sections of the various cold masses. The drawings are to the same scale.

Figure 4 shows a more detailed cross section of one of the 2-in-1 magnets, D4a.

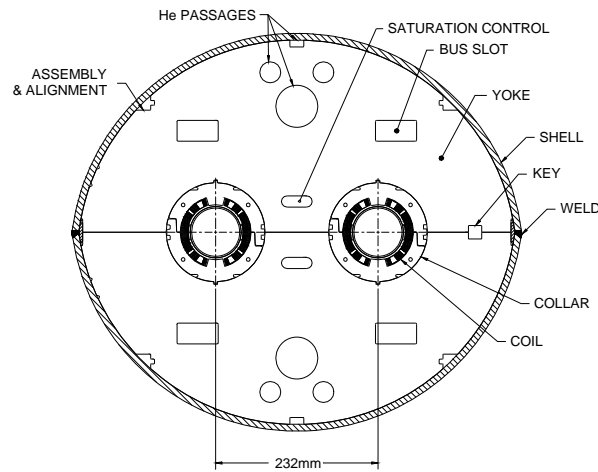


Figure 4 Cross section of the cold mass D4a.

B.3 Assembled Magnets

The cold masses are assembled into cryostats to make completed magnets (see Section C.8). The cryostat consists of a cylindrical vacuum vessel, aluminum heat shield,

blankets of multi-layer thermal insulation, cryogenic pipes, and the magnet support system. A variety of measurements, both mechanical and electrical, will be made on the magnets during the construction process. All subassemblies must satisfy the test requirements before incorporation into a magnet. Completed magnets are tested at cryogenic temperature, then packaged and shipped to CERN for installation into the LHC.

C. Technical Description

C.1 Superconductor

A 30-strand (wire) superconducting cable will be used in the fabrication of all the dipole magnets. A similar cable was used for the RHIC arc dipole and quadrupole magnets [1]. Consequently, the cable fabrication methods are well developed. The superconductor wire to be used in the cable was purchased for the SSC program and has been kept in storage since the end of that project. Its properties are similar to those of the wire used for RHIC, but with a copper to superconductor ratio of 1.8 rather than 2.25. With active quench protection in the magnets, and a sizable margin between required operating current and predicted quench current, it is anticipated that this material will give satisfactory results.

The mechanical and electrical properties of the superconducting wire to be used are summarized in Table 3. Each wire consists of 4165 NbTi alloy superconducting filaments with a nominal diameter of 6 μm and a spacing of $>1 \mu\text{m}$. The exact number of filaments was chosen by the superconductor vendor based on the details of the billet design. Copper is used as the matrix between filaments, it occupies the central core of the wire, and it provides an outer covering for the wire. Copper represents about 64% of the wire cross section and is important for the cable and magnet operational stability as well as for protection against burn-out through overheating during a quench. The wire diameter of 0.648 mm was tightly controlled during final stages of manufacturing and was checked with a laser micrometer.

The wire minimum critical current is defined at a temperature of 4.22 K, an applied magnetic field of 5 T perpendicular to the wire axis and a resistivity of $1 \times 10^{-14} \Omega\cdot\text{m}$ based on the total wire cross section. This current corresponds to a minimum current

density in the NbTi superconductor of 2750 A/mm^2 at 5 T. The SSC wire meets or exceeds this minimum specification. The wire critical current at 3 T will be sampled in order to monitor the effects of superconductor magnetization at low field.

Table 3 Superconducting wire parameters.

Item	Units	Value
Mechanical		
Nominal filament diameter	μm	6
Nominal filament spacing	μm	> 1
Nominal copper to superconductor ratio		$(1.8 \pm 0.1):1$
Number of filaments		4165 ± 20
Wire diameter	mm	0.648 ± 0.003
Wire twist direction		Right
Wire twist pitch	mm	13 ± 1.5
Electrical		
Wire min. critical current at 5 T, 4.2 K	A	325
Wire maximum critical current at 3 T	A	$1.6 \times \text{measured } I_c @ 5 \text{ T}$
Wire maximum R(295 K)	Ω/m	0.082
Wire minimum RRR		38

Thirty wires are fabricated into a Rutherford-type cable by first twisting them around a mandrel, then rolling them into a flat, keystoneed shape with dimensions given in Table 4

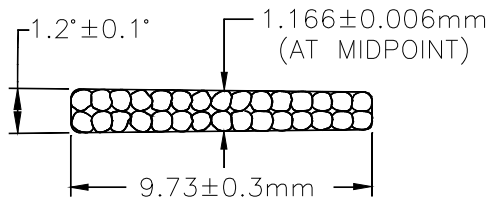


Figure 5 Cross section of the cable to be used to fabricate coils for LHC dipoles.

and Figure 5. The variations of the cable dimensions, especially the cable mid-thickness, will be tightly controlled because the magnetic field quality of the magnets and the coil prestress are dependent on them. The cable lay is chosen to be opposite to the wire twist and requires a cabling machine operating

in a planetary mode for fabrication. The cable minimum critical current (see Table 4) is defined in a similar way to that for the wire, but with the magnetic field perpendicular to the wide surface of the cable and with compensation for self-field. The cable minimum critical current can be obtained from the wire minimum critical current at 5 T times 30 (number of wires in cable) and multiplying by 0.95 (allowance for 5 % degradation in

cabling). Wire piece lengths are large enough to allow all cable lengths to be produced without cold welds.

Table 4 Superconducting cable parameters.

Item	Units	Value
Mechanical		
Number of wires in cable		30
Cable mid-thickness	mm	1.166 ± 0.006
Cable width	mm	9.73 ± 0.03
Cable keystone angle	deg	1.2 ± 0.1
Cable lay direction		Left
Cable lay pitch	mm	74 ± 5
Electrical		
Cable minimum critical current at 5 T, 4.2 K	A	9260
Cable maximum R (295 K)	Ω/m	0.00287
Cable minimum RRR		38

Several differences with respect to RHIC magnets are noted. The cable interstrand resistance may differ from that in the Oxford-produced cable used in the RHIC production magnets. This will change the field distortions due to eddy currents while the magnets are ramped. In addition, the SSC wire to be used has at least some annealing vs. no annealing of the wire used in RHIC (indicated by cable RRR higher than ~ 40). Coils made with this wire are expected to have less post-cure shrinkage than experienced with the RHIC coils, so the coil lengths will be somewhat longer than in RHIC. These differences are not expected to compromise magnet performance in any significant way.

As mentioned, the wire to be used for these magnets was purchased in the SSC program and is now available for the LHC program. Wire from four vendors is available and may be used. In order to study its properties, cable was made from each type of wire, and the properties of the cable were measured [4]. Some results are listed in Table 5.

Table 5 Selected properties of the prototype cable made from wire available to the LHC program. The properties of the available wire are known to vary, however.

Vendor	Cu/SC Ratio	Interstrand Resistance, $\mu\Omega$	I_c , kA (5T, 4.2K)	J_c , A/mm ² (5T, 4.2K)	R, Ω/m (295K)	RRR	Shrinkage,%, 1 hr@225 C
Alsthom	1.87	127	9.651	2770	0.00276	44	0.41

Furukawa	1.76	12	9.949	2762	0.00283	39	0.40
Outokumpu	1.82	14.2	10.448	2983	0.00280	53	0.30
Oxford	1.79	542	10.349	2887	0.00280	45	0.36

C.2 Dipole Beam Tube

The magnets include cold beam tubes with dimensions given in Table 6. Two sizes are required. Magnets that operate at 4.5 K need a larger gap between the beam tube and the coil for effective cooling by the liquid helium [5]. For magnets that require a maximum aperture, a smaller gap can be allowed if the magnets are cooled by superfluid helium (1.9 K).

The tubes are centered inside the coils: horizontally with G-10 bumpers spaced axially at regular intervals, vertically by the collars or by the phenolic spacers in the case of the 1-in-1 magnets. The gap between tube and coil defines a helium buffer space. The tube is seamless, 316 LN stainless steel and is wrapped with 25 μm Kapton with 66% overlay. This provides 75 μm of insulation, which is tested for integrity to ground at 5 kV.

Beam tube liners will be installed into these magnets at CERN. Therefore, except for D1, the tubes do not require copper-plating on the inside surface. Experimental requirements at the LHC require the maximum aperture in two of the D1 magnets, leaving no space for a full length liner. In those magnets, copper-plating will be required to reduce the beam impedance.

Table 6 Dipole beam tube parameters.

Item	Units	Enlarged Tube	Standard Tube
Magnet		D1	D2, D3, D4
Outer diameter	mm	78.00 ± 0.38	73.00 ± 0.38
Outer diameter inc. Kapton wrap	mm	78.1	73.1
Wall thickness	mm	1.96 ± 0.18	1.96 ± 0.18
Inner diameter, nominal	mm	74	69
Weight, nominal	kg	38	34
Beam tube-coil radial gap, nominal	mm	1.0	3.5

C.3 Dipole Coil

The superconducting coil is assembled from two half-coils that are wound on automated machinery and then formed into a specified size in a precision molding operation. It consists of a single layer of 32 turns per half-coil arranged in four blocks with intervening, symmetric copper wedges; the sizes and positions of the wedges and pole spacers give field harmonics that are small (Section C.13). The four current blocks per half-coil design is identified as 9B84A. The cable is insulated with 2 double layers of the polyimide film Kapton CI. The first double layer has polyimide adhesive on the outer side of the film; the second has it on both sides. This all-polyimide insulating system requires a brief exposure to a temperature of 217 °C to set; an appropriate curing cycle was developed and extensively used in the RHIC program with excellent results. The coil ends have been designed to simplify construction and to reduce harmonic content. The number of spacer parts, machined from Ultem, in the two ends of each half-coil totals 27: 17 turn spacers, 2 end saddles, and 8 wedge tips. The coil design parameters are given in Tables 7 and 8.

The coil length given is that of RHIC production coils. As mentioned earlier, the superconductor wire in those coils was “full-hard”, whereas the SSC surplus wire to be used in these coils is “half hard”. This means that it was annealed after wire draw-down. Coils have a tendency to shrink and develop considerable tension during the curing process, so that they become shorter upon removal from the curing mandrel. This is due to tension in the superconducting filaments within the wire, which is developed during wire manufacturing in the draw-down steps, and which is released as the copper anneals during curing. Those that have been made with annealed wire demonstrate less shortening, so the length of these coils for the LHC magnets is expected to be somewhat longer (several millimeters) than given in Table 7.

Table 7 Dipole coil design parameters.

Item	Units	Value
Inner diameter	mm	80
Outer diameter	mm	100
Length, overall	m	9.646
Length, coil straight section	m	9.266
Cable length per half-coil	m	610
Cable mass per half-coil, bare	kg	50

Cable mid-thickness with insulation, under compression	mm	1.352
Dielectric strength: current to ground @ 5 kV	μA	< 200
Coil-collar insulating Kapton thickness, inc. quench resistor	mm	0.64
Midplane Kapton thickness	mm	0.10
Cable wrap material thickness, Kapton CI	μm	25
Pole angle	deg	73.18
Number of turns per half-coil		
1 st block (pole)		4
2 nd block		8
3 rd block		11
4 th block (midplane)		9

Table 8 Coil wedge parameters.

Wedge	Angle, deg	Inner edge thickness, mm	Radial width, mm
1 (pole)	16.68	7.12	9.70
2	9.83	3.09	9.70
3 (midplane)	8.10	0.39	9.65

C.4 Collars

In the 2-in-1 magnets, collars apply mechanical prestress to the coil and separate the coil from the steel yoke. This separation is 10 mm larger than in the 1-in-1 magnets, resulting in reduced saturation effects at high field. In addition, they key the coil to the yoke laminations so that precise alignment of the magnetic field can be set and maintained. The collars are punched from high-manganese stainless steel. This material was used with good results in the SSC program and features high strength, low permeability, and a low thermal coefficient of expansion. The collars are placed around the coil in packs that are ~150 mm long. Sheets of insulating Kapton and quench protection heaters are first placed around the coil, and mid-plane caps of Kapton between coil halves. A press (existing) compresses the collars around the coil. They are held together with phosphor-bronze keys inserted in keyways in the outer surface. The nominal design preload in the coil is 69 MPa at room temperature. This reduces to no less than 33 MPa at cryogenic temperature.

Finite element calculations [6] using ANSYS have established the collar width (the width of the material on the midplane) of 20 mm in the straight section of the magnet. The collars will be spot-welded in pairs as was done in the SSC program. Some

refinements in the design of the collars have been incorporated with respect to the designs used in the SSC program [7]. In particular, the radial gap between the coil and every other collar has been eliminated, a gap that needed brass shims to bridge in order to eliminate damage to the Kapton ground plane insulation. Also eliminated was the interlocking tang/recess feature on the arms of the collars in favor of a simpler shoulder/recess arrangement, made possible by the spot-welded feature.

With a coil compression of 57.9 MPa, the vertical elongation of the collared coil radius is expected to be 75 μm . The Lorentz force at full field results in collar deflections outward in the horizontal direction. After 50-100 μm of radial movement (depending on the actual clearance, nominally line-to-line, between collared coil and yoke inner diameter), the yoke restrains the collared coil and further motion is not possible. Small elastic motions such as these are acceptable and do not compromise quench performance.

In the lead end of the magnet, it is necessary to bring the lead from the pole turn of the coil to the outside over the top of the coil. This is done with a spacer incorporating a path for the cable to follow. Enlarged collars are designed to fit over this spacer. To avoid potentially inadequate support of the coil at the pole in the critical end turn-around, the collars' width is increased from 20 mm to 25 mm. This design results in an enlarged cutout in the yoke, which also has the desired effect of reducing the peak field in the ends. The same yoke cutout is implemented at the return end to maintain symmetry between the ends of the magnet and to reduce the peak field there as well.

With a width of 25 mm, the radial vertical distortion of the end collar is 150 μm under a collaring load of 84 MPa [8]. For most of the end, the modulus of the coil is insufficient to maintain so high a compressive load, so the 150 μm distortion occurs over only a short section of the coil near the pole turn-around.

Figure 6 shows a drawing of the radial construction of the magnet along its length including its two ends. A view of a half-coil including the design for the exit of the lead from the coil pole turn to the outside is shown in Figure 7. The turn is first deflected to the center of the pole, then is ramped up to clear the end turns as it exits the magnets. Parts that fit the geometry and that can be compressed by the collars are used to ensure that the large Lorentz forces exerted on this lead are well constrained. The geometry is difficult because the locations of all parts move as the collars are squeezed onto the coil,

yet the parts must fit with good precision in the assembled magnet if the conductor is to be free of Lorentz motion.

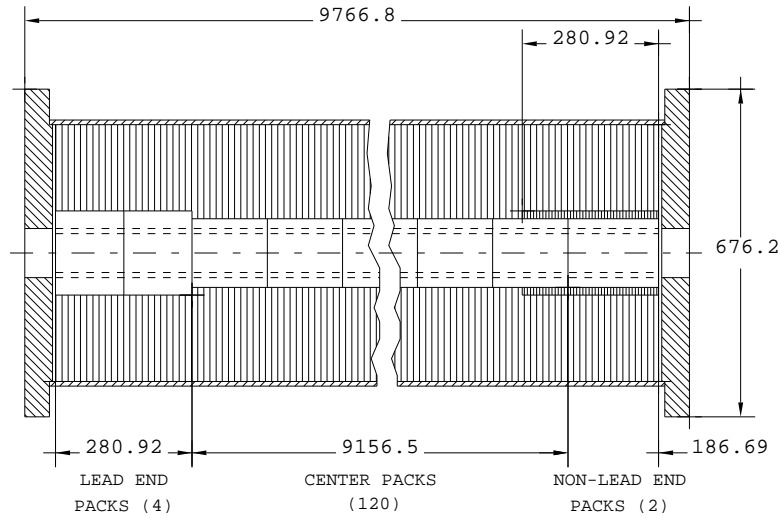


Figure 6 A longitudinal section through one of the apertures of the 2-in-1 magnet, dimensions in mm. The dashed lines near the center indicate the coils, which have an ID of 80 mm and an OD of 101.6 mm. The collars, shown unshaded around the coil, have ODs of 141.6 mm and 173.7 mm in the center and in the lead end respectively. The end plates, which are oval to fit the yoke/shell cross section and have a machined shoulder to accept the round end volume, are shown as they appear on a longitudinal section at the center of the magnet, not at the coil positions.

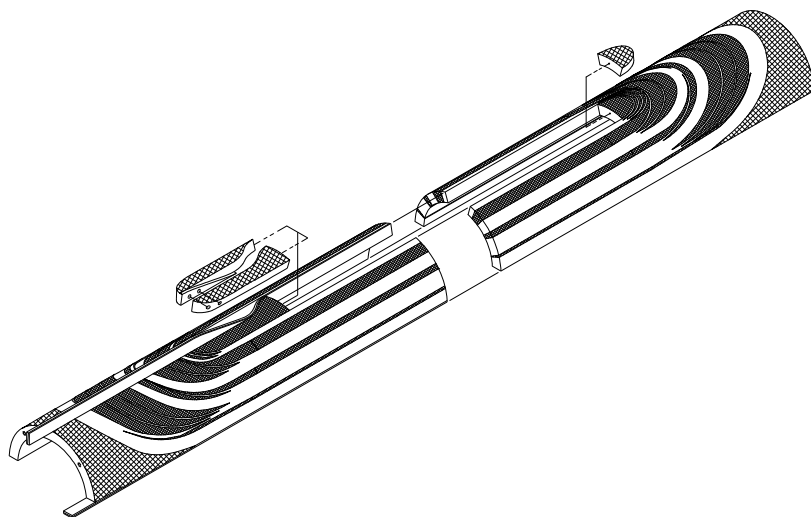


Figure 7 A half-coil showing the leads entering and exiting the coil. The parts guiding the lead from the pole turn to the outside of the coil are especially critical for good performance.

C.5 Dipole Yoke and Helium Containment of the 2-in-1 Magnet

The 2-in-1 yoke is optimized to minimize the current dependence of multipoles at high fields. To reduce saturation-induced harmonics (such as a normal quadrupole term in the dipole), the yoke is made wide enough to contain the flux lines at the maximum design field. Since more iron is required at the midplane, the oblate shape is adopted. This is done by vertically offsetting the center-of-curvature of the half-yoke from the magnet center.

The vertical size is made equal to the LHC dipole yoke outer diameter so that some of its cryostat's hardware can be used. In the present design the yoke outer diameter is 630 mm and, after offsetting the center-of-curvature, the two half-yoke centers, above and below the midplane, are separated by 80 mm. This matches the vertical size of LHC dipoles, which have an outer diameter of 550 mm.

The high field current dependence due to iron saturation is minimized by optimizing the size and location of the saturation control holes or cutouts. In the optimized solution, the computed change in the saturation-induced harmonics (allowed and non-allowed) is within one unit (@ 17 mm radius) in all the dipoles. The saturation is controlled by the various holes placed symmetrically in the yoke, in particular the holes between the two apertures.

Figure 8 shows the flux lines in a 2-in-1 yoke at high field (4 T). As can be seen in the figure, there is ample room in the yoke to contain the flux and little crowding of the flux lines is evident. This explains the low value of the normal quadrupole harmonic at high field, where the left-right asymmetry of the yoke around each aperture might otherwise allow a quadrupole field component to develop.

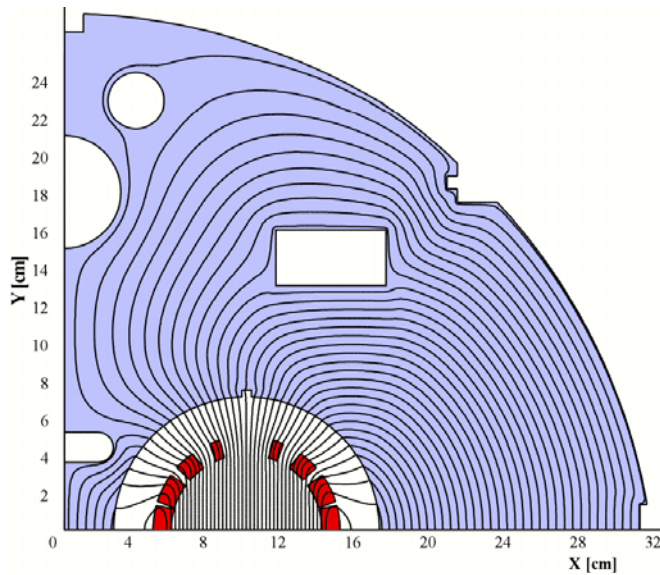


Figure 8 Flux lines in the 2-in-1 magnet. The cutout near the origin increases the reluctance of the flux path on the left, to match that on the right.

The yoke laminations are punched from 1.5 mm thick, low-carbon steel sheet. The desired rms variation for the magnetic field integrated over the length of the dipoles requires that the weight of steel in the yoke be controlled to within 0.07%; to achieve this, the laminations that make up the yoke are weighed and adjusted to this tolerance.

For assembly, the bottom yoke laminations are set up on rails to provide alignment, the two collared coils are placed into the laminations, and the top yoke laminations are placed over the assembly. Stainless steel shells, 9.5 mm thick (designed to meet pressure vessel code requirements), are positioned around the yoke while the yoke is supported through holes in the bottom shell. This support fixture maintains alignment in the subsequent welding operations. The shells are welded together along the horizontal midplane with high manganese-content filler rod [9]. Stainless steel strips fabricated to the required shape back-up the weld (written assembly procedures give the actual sequence of steps required). This welding operation closes the structure and forms a high-pressure (2.1 MPa) helium containment vessel. The shrinkage of the weld compresses the steel yoke and ensures that any residual gap on the yoke midplane is closed. Further compression is provided at operating temperature due to the differential contraction of the stainless steel shell relative to the steel yoke.

The weld back-up strips are shaped to fill the aperture available between the yoke and the shells. A simple bent piece of flat material was originally planned for this strip, but an ANSYS analysis indicated that the shell would develop unacceptable local stresses from a moment around the corner of this cutout when the slot was not filled and the vessel was pressurized at its maximum rating [7].

Following the longitudinal welding of the shell, oval end plates are welded to the shell at each end of the magnet. Set screws that press shaped, stainless steel bars against the ends of the coil are installed in the end plates. They serve to restrain the axial Lorentz forces. The magnitude of these forces determines the thickness of the end plates; the goal, as specified for the RHIC magnets, is typically to prevent deflections in the plate of more than 0.25 mm. According to an ANSYS analysis in which the total Lorentz end force is transmitted to the end plate, the specified end plate thickness of 69.8 mm limits the deflection to 0.125 mm [7].

Additional operations on the cold mass include the welding of closure plates over the alignment holes in the shell and the attachment of cradles to support the cold mass on posts in the cryostat. After completion of electrical interconnect work at the ends of the magnets, cylindrical end bells with domed ends are mounted on machined shoulders and welded to the oval end plates to close the helium volume and to make the transition to the neighboring magnet or cryo-module.

Some yoke design parameters are listed in Table 9. For comparison, the RHIC dipole parameters (original design operating field was 3.4 T) are also listed.

Table 9 Dipole yoke and yoke containment design parameters.

Item	Units	Value	
		1-in-1 (RHIC)	2-in-1 (LHC)
Aperture for collared coil	mm	119.4	141.6
Yoke horizontal size	mm	266.7	625
Yoke vertical size	mm	266.7	550
Lamination length	m	9.64	9.64
Length inc. end plates	m	9.72	9.79
Overall length	m	10.23	10.35
Weight of steel	kg	2,757	16,700

Shell, wall thickness	mm	4.8	9.5
Shell, weight	kg	306	1340
End plate, thickness	mm	31.8	69.8
End plate, weight	kg	18	110
Cold mass weight	kg	3,607	19,200

C.6 Analysis of the Collar-Yoke and the Yoke-Shell Interfaces

In the assembly of the yoke around the collared coil, it is important that the dimensions and tolerances be well controlled so that yoke closure is assured. Gaps of more than $\sim 50 \mu\text{m}$ on the yoke midplane could lead to undesirable harmonics. A number of design features have been incorporated to address this concern. First, the keyway position on the collar laminations has been offset to yield a round collar after keying at the minimum expected coil stress of 57.9 MPa. An ANSYS analysis has determined that this radial deflection after collaring will be $75 \mu\text{m}$. As an additional precaution, an assortment of collaring keys will be available for the prototype magnets. Measurements will be taken to determine the actual collar diameters after keying and the key size will be adjusted to minimize the ovality. Independent adjustments will be made to the lead end, straight section and non-lead end collars. Changes in the size of the pole and midplane shims can be made in the prototype, if necessary, in order to maintain the proper pre-stress.

A tolerance analysis was performed to determine the maximum possible yoke midplane gap on subsequent production magnets, once the preceding optimization on the prototype is complete [10]. Tolerances on the collar outside diameter, keyway position, key thickness, yoke inside diameter, and yoke ID position were considered. Variations in collar outer diameter due to variations in coil size/stress were also included. The maximum possible yoke midplane gap prior to shell welding was found to be 0.3 mm. It is expected that such a gap would be eliminated as a result of stresses developed in the shells during welding. Measurements will be made on the production magnets to verify this expectation.

C.7 Electrical Connections and Quench Protection

The electrical connections to the magnets will be made with the usual convention in which current into the positive or “A” lead produces a normal dipole field with the South pole at the top. Definitions and conventions used at Brookhaven in the building and measuring of magnets are given in [11].

The bus conductor for each magnet and its immediate neighbors is placed inside an insulating conduit that is then installed as a completed package into the bus slots of the yoke, typically at the bottom. The electrical connections between bus conductors and magnet leads are at the ends of the magnets, within the end volume contained between the stainless steel magnet end plate and the end of the magnet cold mass. This end volume also contains the thermal expansion joints for the bus conductors. These will follow BNL designs as developed for RHIC. No magnet warm-up heaters to accelerate the occasional warm-up of the cold mass are planned; warm gas only is used for warm-up in the LHC

Quench protection heaters are used to protect the coils from excessive local energy deposition during a quench. The basic heater design was developed and extensively tested by BNL in the SSC program. The heaters run the full length of the magnet, one per quadrant, and are installed between the collars and coils at the time of coil assembly for collaring. Two independent circuits per magnet are included. In operation, these magnets will be connected in series and the quench protection system will, when triggered, fire one of these independent heater circuits in all the magnets (up to 4 apertures).

Until measurements are made on a prototype magnet, it is not possible to predict exactly the temperature that will be reached in a coil during a quench. The active quench protection system being planned for these dipoles will result in much lower peak quench temperatures than is the case in the similar RHIC dipoles, which are protected with diodes only, even though the conductor in these magnets will contain less copper. In the RHIC program, measurements were made of $\int I^2 dt$ (10^6 A² sec or MIITS) versus temperature for a preliminary version of a RHIC dipole. This enabled calibration of a model used for predicting the quench margins in the final version of the RHIC dipole. Final estimates of worst case $\int I^2 dt$ values in RHIC magnets for conductor with a copper-to-superconductor ratio (Cu:SC) of 2.25:1 and a single quench protection diode for each

magnet gave a value of about 12.4 MIITS, compared with an estimated cable damage level of 13.8 MIITS. This converts to a temperature margin of about 250 K before the damage temperature of 835 K is reached. This damage temperature was measured in earlier experiments on full sized magnets at Brookhaven.

C.8 Dipole Cryostats

The cryostats for D2, D3 and D4 will be the same as those for the main LHC dipoles [12] wherever possible (D1 is housed in a RHIC-design cryostat). The lengths will be different (shorter), the support points for the cold mass will be adjusted, and the support cradles will be designed to accommodate the dual 1-in-1 or the 2-in-1 cold masses, but the diameter of the vacuum tank, the support posts [13], and the heat shield support extrusions will be the same. A substantial amount of bus work that services the magnets in the adjacent LHC arc passes through the D4 magnets. It is planned that this bus work will be placed in a separate tube in the cryostat. Drawings of the various cryostatted magnets are shown in the following Figures 9 to 12.

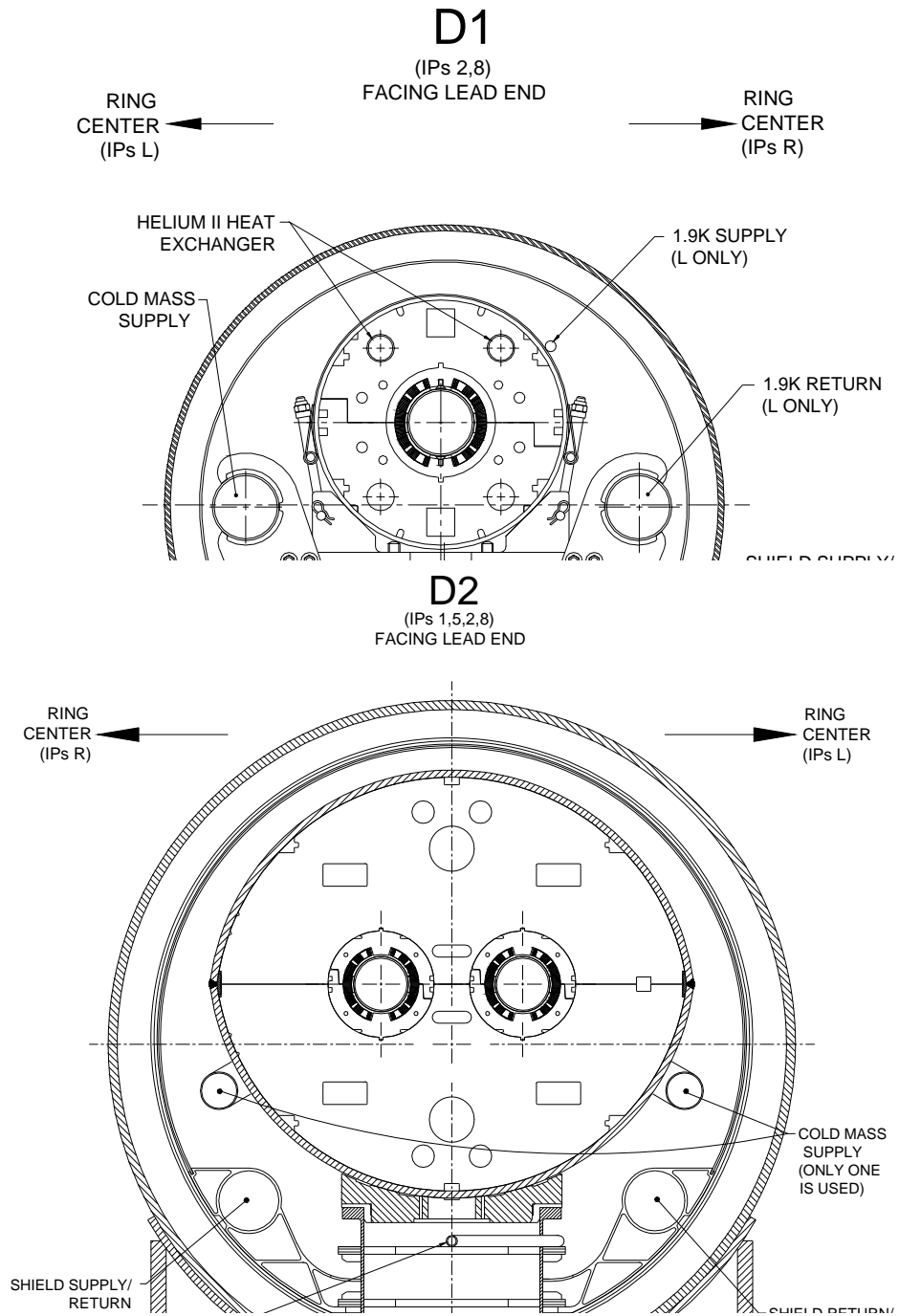


Figure 9 Cross section of D1.

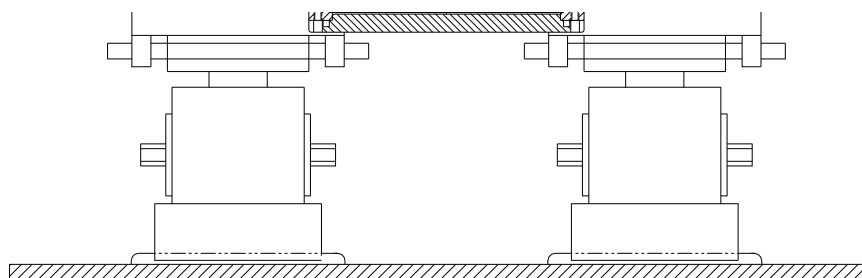


Figure 10 Cross section of D2.

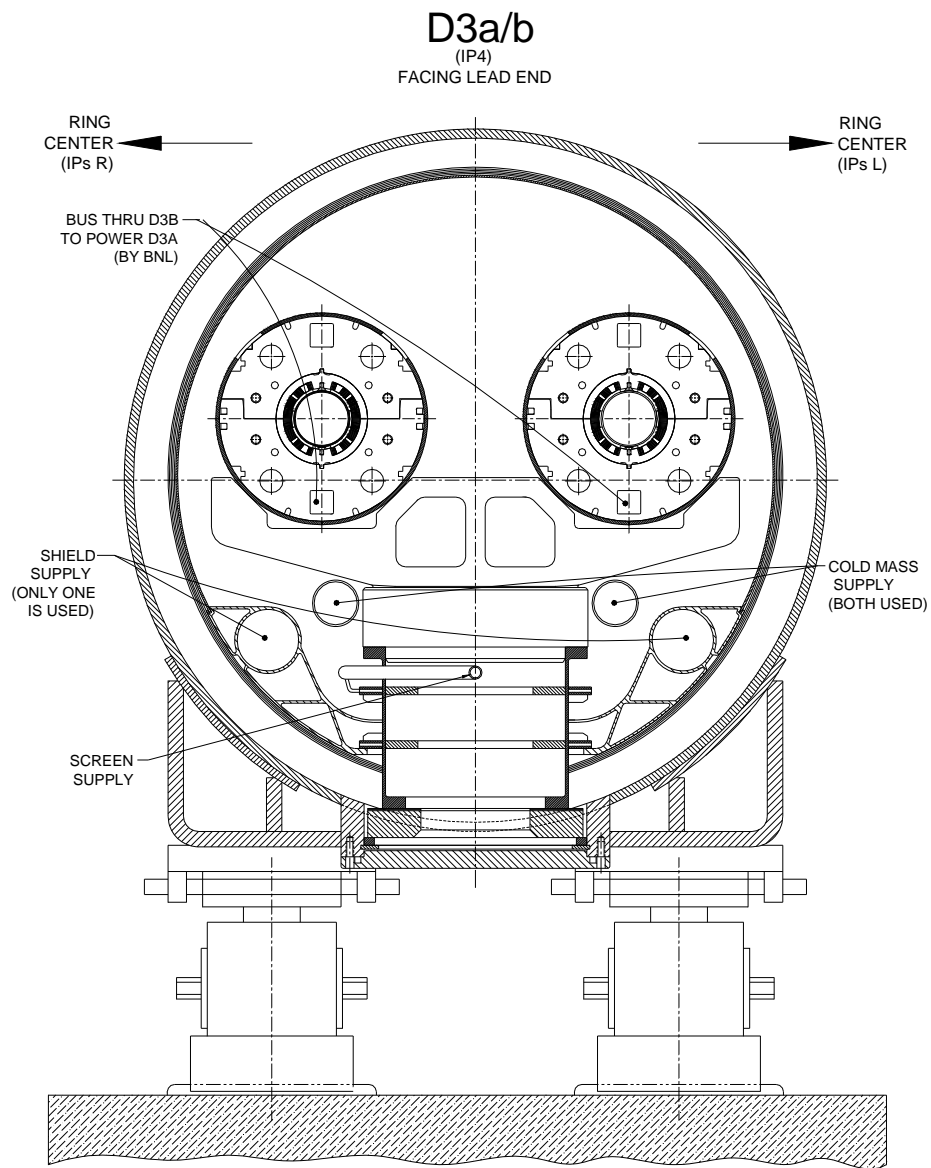


Figure 11 Cross section of D3.

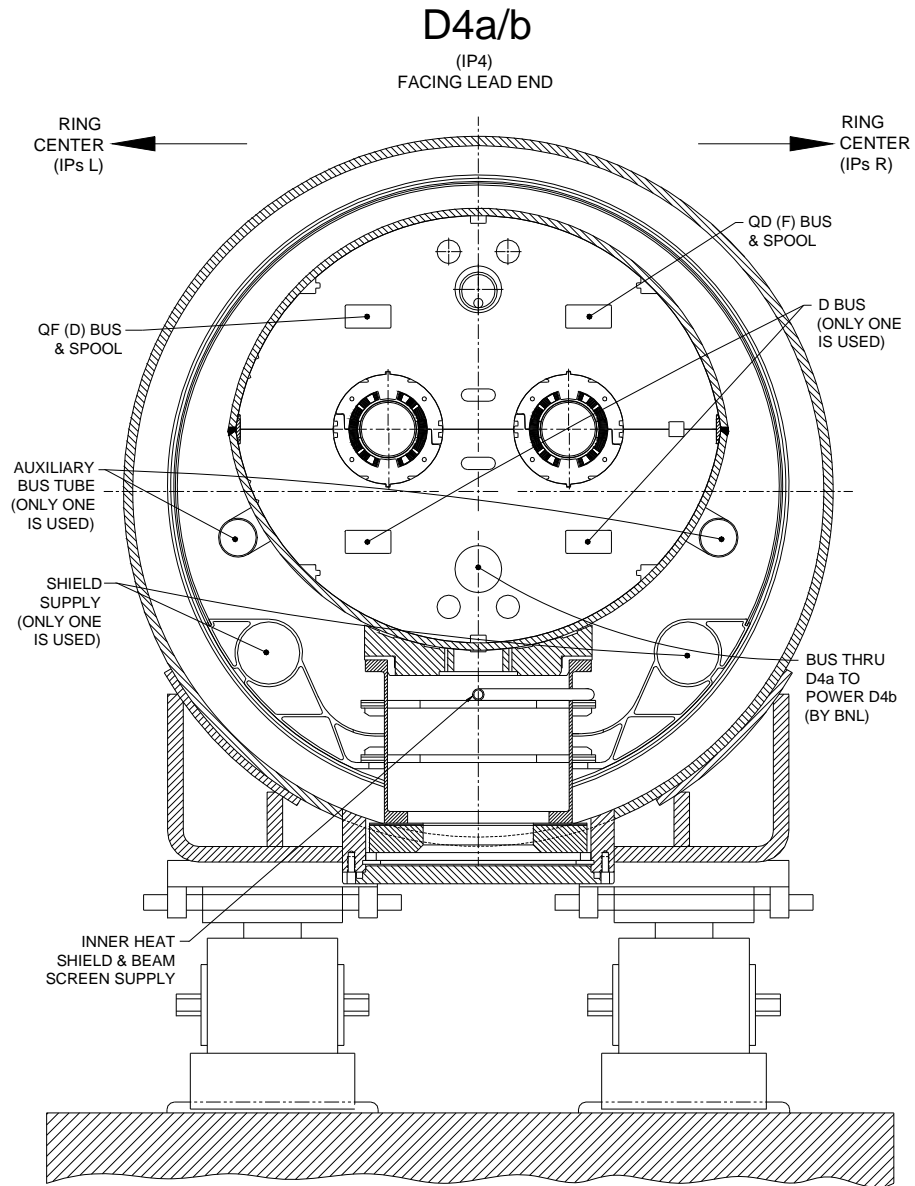


Figure 12 Cross section of D4.

C.9 Interfaces to LHC Systems and Magnet Cooling

Each magnet that is delivered by BNL to CERN must fit correctly into a predetermined slot and must be so configured that connection to the LHC cryogenic and electrical system is facilitated. This requires a great deal of careful design work and back-and-forth communication with the staff at CERN. The present plans for these interfaces are given in reports by S. Plate [14] and K. C. Wu [15].

The dipoles will operate either in a static bath of liquid helium at 4.5 K or in a static bath of superfluid helium at 1.9 K (see Table 1). The operating temperature is determined by the logistics of position in the lattice of the LHC. Depending on position in the LHC and the operating temperature, provision must be made in the magnets constructed at BNL for the correct interfaces, pipes and controls in each magnet. Typical schematics are shown in Fig. 13 for D4 operating at 1.9 K and in Fig. 14 for D3 operating at 4.5 K.

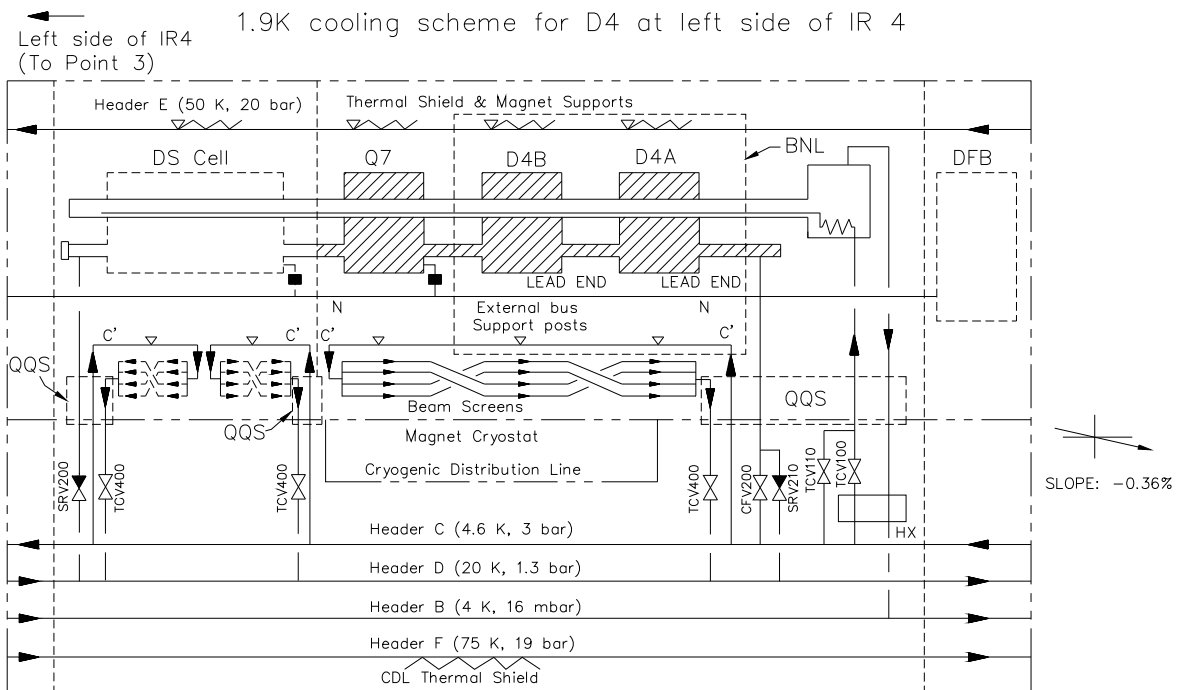


Figure 13 Drawing of the cryogenic connections for D4 on the left side of IR4.

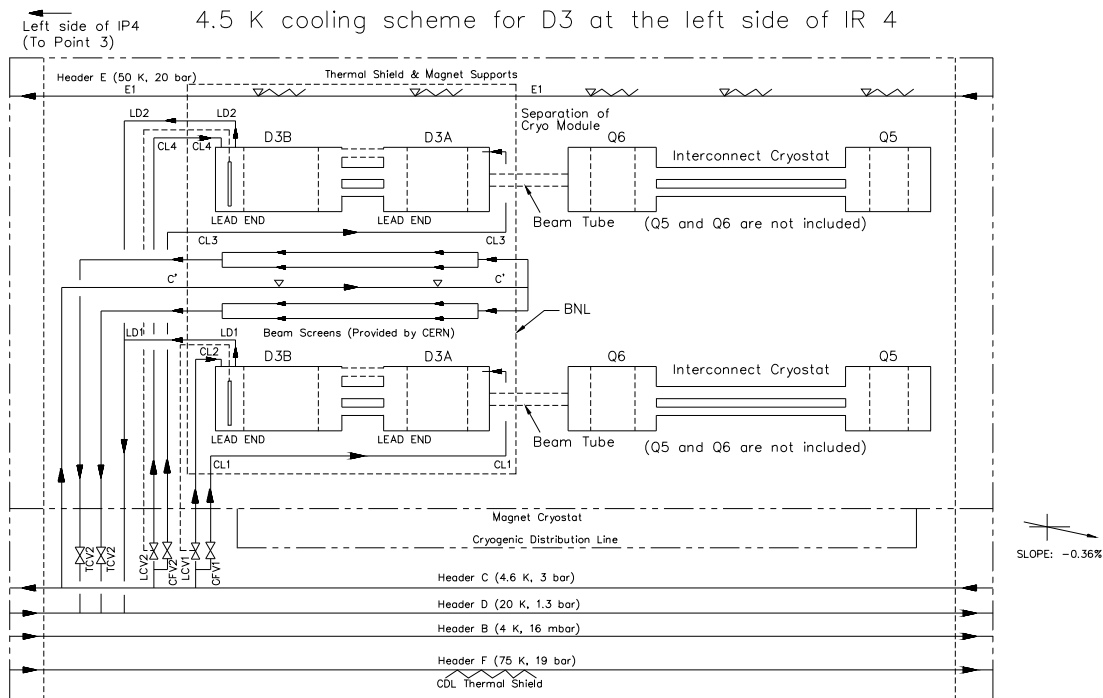


Figure 14 Drawing of the cryogenic connections for D3 on the left side of IR4.

There are a number of design features that are observed in the systems operating with a static bath of helium at 4.5 K so that they will function properly in the LHC, including the following:

- Transfer liquid helium to the high elevation end for the make-up fill.
- Transfer liquid helium to the low elevation end for the initial fill.
- Allow helium vapor to return to the high elevation end through the helium containment of the magnet, mostly through the two upper helium passages.
- Use the lower bus openings in the magnet for the superconducting bus.
- Install a level gauge in the end volume to control helium flow and keep magnet coil and bus in the liquid region.

C.10 Transfer Function, Quench Field, Inductance, and Stored Energy

A plot of the expected field vs. current in the 2-in-1 dipole magnet D4b is shown in Figure 15. The field is 3.8 T at 6030 A (0.630 T/kA). The quench field ($T = 4.5$ K) is expected to be 4.8 T at a current of 7740 A, assuming conductor with a short sample limit of 2750 A/mm^2 at 5 T, 4.2 K. The current density in the copper at the quench point is 1218 A/mm^2 . The inductance of each aperture is 25.8 mH and the stored energy in each aperture at 3.8 T is 470 kJ.

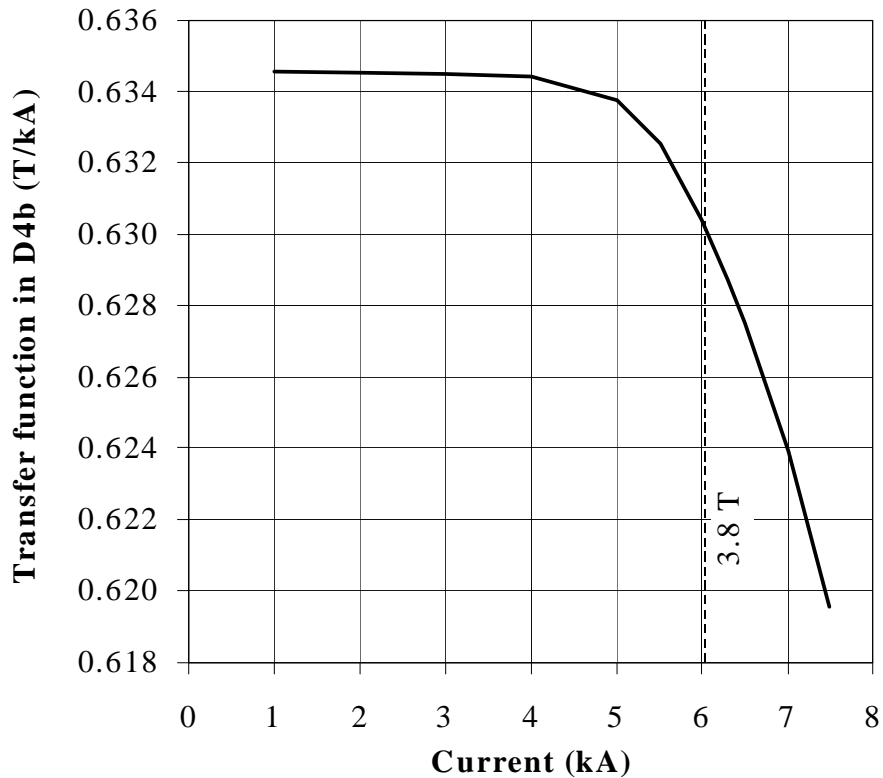


Figure 15 Transfer function for the 2-in-1 dipole D4b.

Because of their differing yoke designs, each of the magnets will have a slightly different field vs. current transfer function. Fig. 16 shows the dipole field as a function of

current in the various magnet types. Figure 17 shows the currents relative to D3a for the same field in the different magnets.

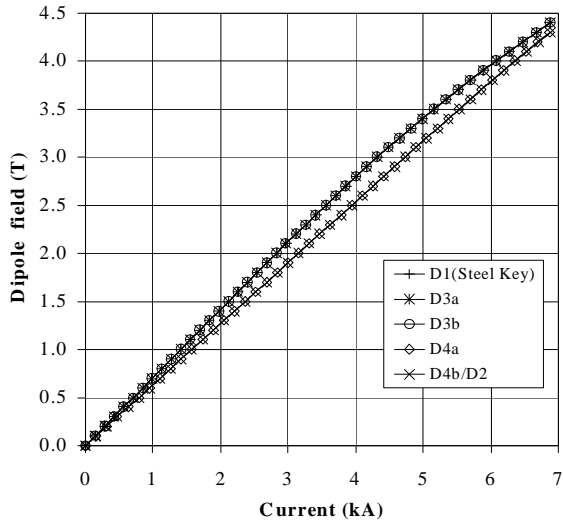


Figure 16 Field vs. current for the various magnets.

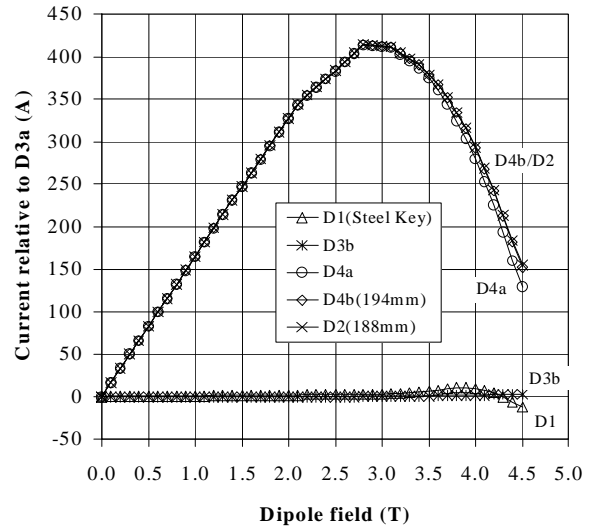


Figure 17 Current relative to D3a for a particular field in the various magnets.

C.11 Magnetic Field Quality - Measurements

Warm magnetic measurements to determine field multipoles will be made when magnet construction has been completed, including all welding and installation into the cryostat. This will allow detection of errors in magnet construction that may not have been detected in the earlier construction testing. Except for small systematic offsets in the lower allowed multipoles, warm field measurements have been shown to be closely related to the field multipoles measured when the magnet is cold. The data will be examined for conformance to expected field quality. This includes the dipole field angle orientation, the integral of the magnet's dipole field, the multipole content of the field, and the variations of the field parameters along the length of the magnet. Just as for the RHIC dipoles, it is anticipated that all magnets properly built to print will easily pass the field quality test, and that only a magnet with construction deficiencies will fail to pass the test. Following the warm tests, cold testing will be done on each magnet in Brookhaven's Horizontal Test Facility to check quench performance and to verify field

quality. Magnets operating in static liquid helium in the LHC will be tested with the planned slope under the same conditions at BNL. Since the BNL facility does not operate at 1.9 K, those that operate at 1.9 K in the LHC will be tested with supercritical forced flow (5 bar, 4.5 K) at BNL.

The MOLE measuring system [16] developed at BNL and used for RHIC field measurements will be used for the LHC magnets. Integral fields will be measured with the stationary integral coil system [17] used for RHIC magnets.

C.12 Magnetic Field Quality – Measurement Errors

The extensive measuring program carried out for RHIC magnets has given data that can be analyzed for systematic and random measurement errors. Such an analysis has been carried out, including also an analysis of errors in the calibration of the measuring coils. The analysis has been summarized in a series of tables and plots [18]. Table 10 is excerpted from the report. For clarity, the reference radius is 25 mm as in the report. These errors apply to the measurement system used for the RHIC arc dipole measurements, which will be used for these magnets, and will be different for other measuring systems. They are, however, a good benchmark for the accuracy that can be achieved in a carefully built and calibrated system.

Table 10 Estimated measurement errors. δ is the maximum error due to measuring coil construction/calibration, given as a percent of the value of the harmonic. $\sigma(b_n)$ and $\sigma(a_n)$ are the random errors in the measurements. $\Delta(b_n)$ and $\Delta(a_n)$ are the suggested values for the total measurement errors for magnets with small harmonics as in the RHIC dipoles. These include also some variations due to magnet changes after quench and/or thermal cycles as seen in the RHIC magnets. They are obtained by rounding the sum of the effects of all expected error sources upward and by specifying minimum values for several of the harmonics. Note: sextupole is $n=3$, σ and Δ in units (parts * 10^{-4} of the central field), reference radius=25 mm.

n	δ, %	$\sigma(b_n)$, units	$\Delta(b_n)$, units	$\sigma(a_n)$, units	$\Delta(a_n)$, units
2	0.48	0.061	0.10	0.043	0.50
3	0.78	0.033	0.50	0.015	0.05
4	1.08	0.012	0.05	0.010	0.10
5	1.38	0.004	0.10	0.005	0.02
6	1.68	0.003	0.02	0.004	0.05
7	1.98	0.002	0.02	0.002	0.02
8	2.28	0.001	0.02	0.002	0.02
9	2.59	0.001	0.02	0.001	0.02
10	2.89	0.001	0.02	0.001	0.02
11	3.19	0.001	0.05	0.001	0.02

C.13 Magnetic Field Quality – Expected Values

The magnets are designed to have harmonics that are small. Thus, the geometric multipoles (harmonics) are expected to be near zero. At low fields, persistent currents in the superconductor will generate normal sextupole (b_3) and decapole (b_5) components. These as well as the normal 14-pole (b_7) are shown in Figure 18. The harmonics were measured in the RHIC dipole DRG107. At high fields, some harmonics will be induced by the saturation of the iron yoke, as shown in Figure 19.

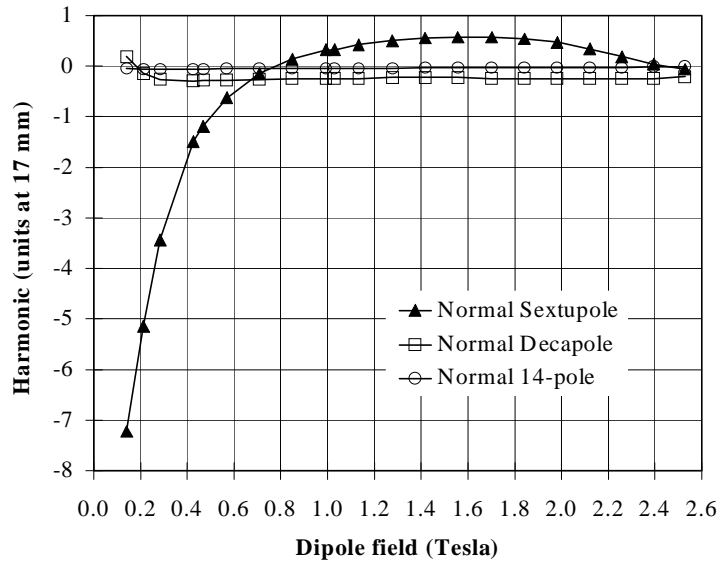


Figure 18 The measured dependence of the sextupole, decapole and 14-pole harmonics on field during up-ramp in the 80 mm aperture RHIC arc dipole DRG107. At low fields, the value of the sextupole harmonic (b_3) is dominated by the persistent currents.

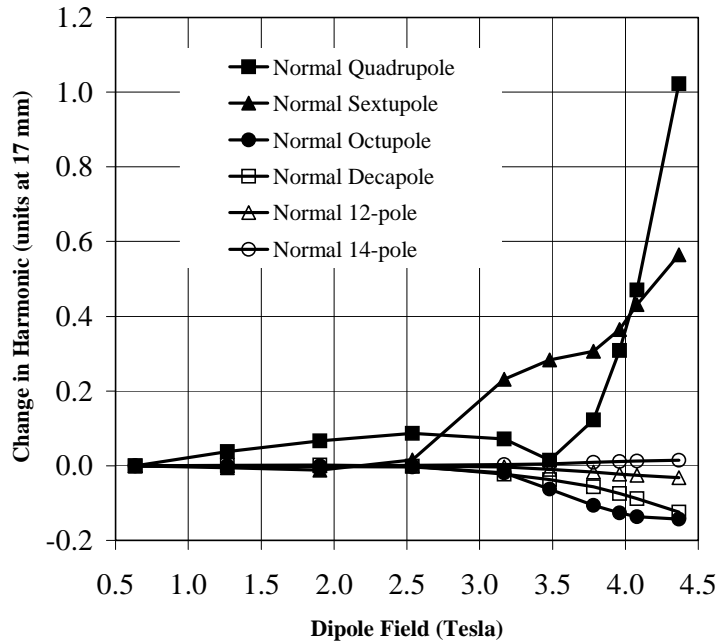


Figure 19 The computed current dependence of the field harmonics in an aperture of dipole D2. The maximum operating field in the magnets is 3.8 T.

Field integral and field angle errors in the 2-in-1 dipoles, based on RHIC magnets [1,2], are given in Table 11.

Table 11 Estimated errors on integral field and field angle.

Item	Value
Integral field, magnet-to-magnet variation, rms	5×10^{-4}
Single magnet, mean dipole angle, α	± 3 mrad
Single magnet, variation (twist) of dipole angle $\Delta\alpha$ from mean, rms	2 mrad
Mean angle between apertures, rms	2 mrad

The measured harmonics in the magnets may be non-zero due to design and construction errors. The estimated integral values of field harmonics and their errors in D4a are given in Table 12 [19]. The saturation-induced harmonics are so small that they are included in the uncertainty in the mean; this is true in the other dipole designs as well. The estimated value of the persistent current-induced sextupole harmonic around injection (~ 0.3 kA or ~ 0.2 T) is -6 units.

Table 12 Expected integral harmonics at 3.8 T in the D4a magnets. b_n and a_n are the expected means of the normal and skew terms due to geometry. $\delta(b_n)$ and $\delta(a_n)$ are the combination of (i) the uncertainty in the mean and (ii) the saturation induced harmonics. $\sigma(b_n)$ and $\sigma(a_n)$ are the expected random variations. Note: sextupole is $n=3$, ref. radius 17 mm.

n	b_n, units	$\delta(b_n)$, units	$\sigma(b_n)$, units	a_n, units	$\delta(a_n)$, units	$\sigma(a_n)$, units
2	0.03	0.54	0.19	0.36	2.52	1.03
3	1.06	1.65	0.79	-0.49	0.25	0.08
4	-0.02	0.07	0.03	0.02	0.34	0.13
5	-0.02	0.17	0.08	0.04	0.04	0.01
6	0.00	0.01	0.01	0.00	0.08	0.02
7	0.00	0.02	0.01	-0.01	0.01	0.00
9	0.00	0.01	0.00	0.00	0.00	0.00
11	-0.01	0.00	0.00	0.00	0.00	0.00

The field errors in the magnets (which are based on the already excellent RHIC field quality) may be somewhat smaller than given here because the replacement of RX630 phenolic spacers with punched stainless steel collars will result in smaller dimensional

variations. Nevertheless, techniques for adjusting the field harmonics by small amounts have been developed in recent years [20]. These include coil size adjustment during cure, adjustment of coil midplane and pole shims, and coil wedge thickness adjustment. Changes can be made if field measurements on the first one or several magnets indicate, through tracking studies, that such adjustment would be appropriate. These techniques will be available for use on the magnets as needed.

The non-zero skew quadrupole term a_2 results from a warm-cold shift upon cool down and is not explained. The non-zero values of the skew terms a_3 , a_5 , etc. are primarily from the harmonics in the lead end, as measured in the RHIC arc dipoles. In a single layer coil design such as used in these dipoles, there are leads carrying the current into and out of the coil that cannot be paired at every point. These leads, particularly the lead at the pole, produce a low level of skew harmonics in the lead end field. In addition, some normal allowed harmonics are generated in the ends of a single layer coil because it is not possible to completely balance the opposite multipoles generated by current turns near the midplane vs. current turns near the pole in the end region of the magnet.

C.14 Current Imbalance in the Left/Right Apertures

For various reasons, the 2-in-1 magnet D2 may be operated with a small current imbalance in one aperture with respect to its neighboring aperture. The following Figure 20 shows the effect of such an imbalance on the fields in the magnet. In these calculations, 15 % additional current is assumed in the left aperture and the field changes in both the left and the right apertures are then plotted as a function of field in the right aperture. The effects for both D4b, which has an aperture separation of 194 mm, and D2, with an aperture separation of 188 mm, are shown and are small. At 4 T, the maximum difference in left/right harmonics is ~ 3 units for the sextupole term. The transfer function difference is less than 0.1 %.

× D4B(194mm): Rev.A Yoke; Cur(Left) =1.15*Cur(Right); D4BA2APLMORE2; Harmonics at 17mm in Right Aperture
 □ D2(188mm): Rev.A Yoke; Cur(Left) =1.15*Cur(Right); D2A2APLMORE2; Harmonics at 17mm in Right Aperture
 △ D4B(194mm): Rev.A Yoke; Cur(Left) =1.15*Cur(Right); D4BA2APLMORE2; Harmonics at 17mm in Left Aperture
 ○ D2(188mm): Rev.A Yoke; Cur(Left) =1.15*Cur(Right); D2A2APLMORE2; Harmonics at 17mm in Left Aperture

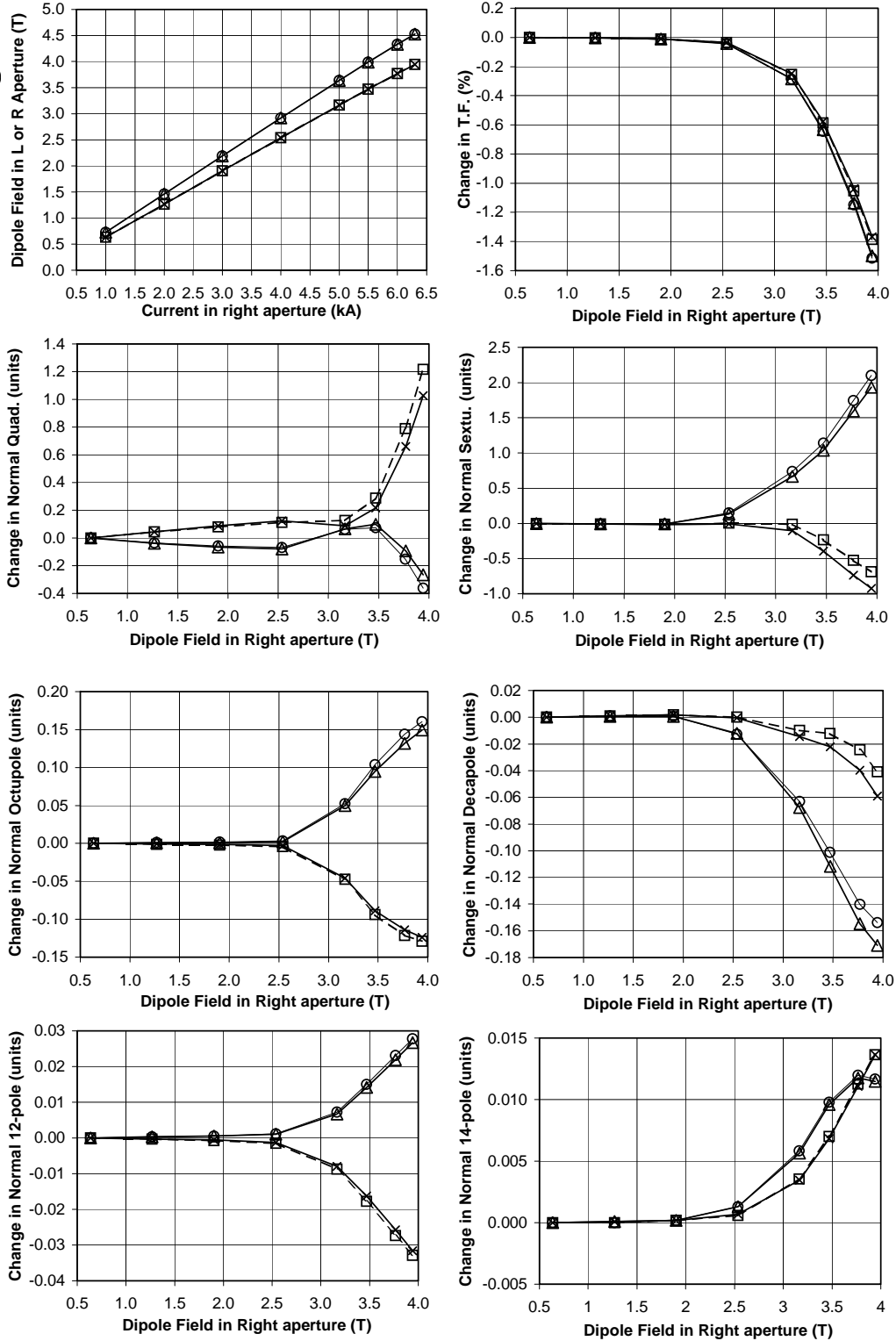


Figure 20 Change in harmonics with a 15 % current imbalance in the apertures of the 2-in-1 magnets D2 and D4b.

C.15 Magnet Shipping

Once construction and testing of the magnets is complete, they will be shipped to CERN for installation into the LHC. To prepare them for transit, steel support posts and end restraining frames will be installed to protect the cold mass support posts from damage. The magnets will be sealed and filled with dry nitrogen so that moisture cannot penetrate the cryostat or cold mass. Each magnet will be mounted on a shock-absorbing frame and then placed into a standard 40-foot-long shipping container. This container will be transported by truck to a shipping terminal, then by ocean freight to a terminal in Europe, then by truck to CERN. The frames will be returned to BNL for reuse. The production rate is low enough that only two such frames are necessary for this program.

C.16 Installation at CERN

CERN personnel will install the magnets into the LHC lattice. They must be placed on stands supplied by CERN, and surveyed into place. The beam tube liner must be installed, internal wiring and pipe connections to a QQS module must be made, the several volumes welded shut, and various leak checks and pressure checks carried out. CERN test apparatus will be required to verify that the magnets have survived the trip and are behaving up to specification. At this stage, the magnets become the responsibility of CERN as that laboratory brings the LHC into operation.

D. R&D Program

Because the superconducting coils planned for these magnets are the same as those used in the RHIC dipole magnets, the required R&D program is reduced in scope from that normally required to develop a new design of superconducting magnet. Two short 2-in-1 models, each ~ 3 m long, will be built and tested in vertical dewars, with the following goals:

1. Qualify tooling and construction techniques.
2. Confirm the proper fit of all mechanical components.
3. Monitor the coil prestress at room temperature and at cryogenic temperature using strain gauges.
4. Check quench performance and field margin.

5. Measure magnetic field for possible iteration of coil design to achieve the desired field uniformity.
6. Check performance of quench protection heaters.
7. Measure temperature rise in coil for quenches at various current levels using a system of voltage taps and spot heaters.

E. Production Plan and Schedule

Magnet production will take place at BNL in the buildings and facilities that were used for RHIC magnet production, which ended in 1998. These facilities will be reconfigured to build spare RHIC magnets as required, and the LHC magnet production will share the space and manpower assigned to that work. The LHC production has been planned earlier than required to meet CERN schedules. This was done to match the available spending profile in the US accelerator program. The schedule for dipole magnet production is shown in Figure 21.

Schedule for LHC Magnets																													
Schedule of May 18, 1999		FY 1997				FY 1998				FY 1999				FY 2000				FY 2001				FY 2002				FY 2003			
		1	2	3	4	1	2	3	4	1	2	3	4	1	2	3	4	1	2	3	4	1	2	3	4	1	2	3	4
1.1.2. Interaction Region Dipoles																													
Engineering and design		-----																											
Tooling mods for D1																													
Manufacture superconducting cable																													
Deliverables																													
Purchase material																													
Magnet construction																													
D1 (IR2 & IR8) - 5 ea.																													
D2 (IR1, IR2, IR5, & IR8) - 9 ea.																													
Total																													
1.2.1. RF Region Dipoles																													
Engineering and design		-----																											
Tooling, inc test coils																													
Manufacture superconducting cable																													
Prototypes: D4b - 2 ea																													
Purchase material																													
Manufacture D4b #1 Begin 7/6/99																													
Manufacture D4b #2 Begin 7/19/99																													
Test D4b #1 Nov, '99																													
Test D4b #2 Jan, '00																													
Deliverables																													
Purchase material																													
Magnet production																													
D3a - 3 ea.																													
D3b - 3 ea.																													
D4a - 3 ea.																													
D4b - 3 ea.																													
Total																													

Figure 21 Schedule for building the magnets. The number of magnets to be delivered each quarter is shown.

References

- [1] RHIC Design Manual, Brookhaven National Laboratory.
- [2] E. Willen, Superconducting Magnets, BNL 64183.
- [3] V. Ptitsin, S. Tepikian, J. Wei, BNL-Built LHC Magnet Error Impact Analysis, RHIC/AP/174.
- [4] A. Ghosh, Report on SSC-Purchased Superconducting Wire Proposed for the LHC Magnets, BNL Magnet Note 581, April 22, 1999. Shrinkage measurements courtesy of CERN.
- [5] M. Rehak, R. Shutt, Pressure Drops and Temperature Increases in RHIC Magnets, BNL Magnet Division Note 423, March 4, 1992.
- [6] R. Alforque, LHC Magnet Central Collar, http://dekooning.cad.bnl.gov/design_safety/notes, Number 9.
- [7] M. Anerella, Presentation to the Dipole Magnet Conceptual Design Review, BNL, July 16, 1998.
- [8] R. Alforque, LHC Magnet End Collar, Rev.1, http://dekooning.cad.bnl.gov/design_safety/notes, Number 12.
- [9] Weld wire type ER385L, with nitrogen and manganese enhancement.
- [10] J. Schmalzle, LHC 2-in-1 Dipole-Yoke Midplane Gap, BNL Magnet Note 577, September 17, 1998.
- [11] A. Jain, F. Dell, S. Peggs, D. Trbojevic, P. Wanderer, J. Wei, RHIC Magnetic Measurements: Definitions and Conventions, BNL Magnet Note 562, January 29, 1997.
- [12] J.C. Brunet, V. Parma, G. Peñn, A. Poncet, P. Rohmig, B. Skoczen, L.R. Williams, Design of the Second Series 15 m LHC Prototype Dipole Magnet Cryostats, LHC Project Report 133.
- [13] M. Mathieu, T. Renaglia, C. Disdier, Supporting System for the LHC Cold Mass, LHC Project Report 139.
- [14] S. Plate, Configurations of BNL-Built LHC Dipole Magnets, in process.
- [15] K. C. Wu, S. R. Plate, E. H. Willen, Cooling Scheme for BNL-Built LHC Magnets, in process.
- [16] G. Ganetis, J. Herrera, R. Hogue, J. Skaritka, P. Wanderer, E. Willen, Field Measuring Probe for SSC Magnets, Proc. 1987 PAC, Washington, DC, March, 1987.
- [17] A. Jain, Field Quality Measurements in RHIC Dipoles, Proc. 9th Int. Mag. Meas. Workshop, Vol. 1, Saclay, June 19-22, 1995.
- [18] A. Jain, Estimation of Errors in the Measurement of Harmonics in RHIC Arc Dipoles, Magnet Group Note 570, Brookhaven, November 18, 1997, <http://magnets.rhic.bnl.gov/publications.htm>.
- [19] A. Jain, R. Gupta, P. Wanderer, E. Willen, Magnetic Design of Dipoles for LHC Insertion Region, EPAC98, June 1998, <http://www.cern.ch/accelconf/e98/PAPERS/TUP03F.PDF>.
- [20] R. Gupta, Estimating and Adjusting Field Quality in Superconducting Accelerator Magnets, Proceedings of the LHC Collective Effects Workshop, Montreux, 1995, published in Particle Accelerators, **55**, [375-385]/129-139, 1996, and BNL Report 62952.